AD-A037 386 ARMY ELECTRONICS COMMAND FORT MONMOUTH N J F/G 20/5
A HIGHLY-STRESSED CYLINDRICAL ELECTRODE CARBON DIOXIDE (CO2) TR--ETC(U)
FEB 77 G R OSCHE, H W SONNTAG

UNCLASSIFIED ECOM-4468 NL

| OF |
ADA037386

END

DATE
FILMED
4-77

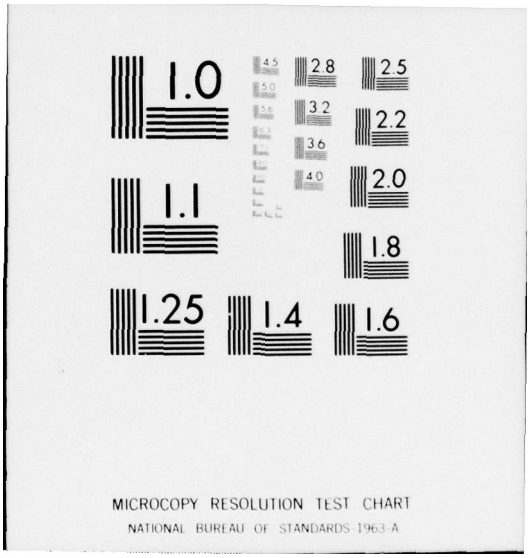
1.0
1.1
1.25
1.4
1.6
1.8
2.0
2.2
2.5
2.8
3.2
3.6
4.0
4.5
5.0
5.6
MICROCOPY RESOLUTION TEST CHART
NATIONAL BUREAU OF STANDARDS-1963-A

Research and Development Technical Report

ECOM - 4468

A HIGHLY-STRESSED CYLINDRICAL ELECTRODE CARBON DIOXIDE (CO_2) TRANSVERSELY EXCITED ATMOSPHERIC (TEA) LASER

G. R. Osche
H. E. Sonntag

Combat Surveillance & Target Acquisition Laboratory

February 1977

ECOM

US ARMY ELECTRONICS COMMAND FORT MONMOUTH, NEW JERSEY 07703

NOTICES

Disclaimers

The findings in this report are not to be construed as an official Department of the Army position, unless so designated by other authorized documents.

The citation of trade names and names of manufacturers in this report is not to be construed as official Government indorsement or approval of commercial products or services referenced herein.

Disposition

Destroy this report when it is no longer needed. Do not return it to the originator.

UNCLASSIFIED

SECURITY CLASSIFICATION OF THIS PAGE (When Data Entered)

REPORT DOCUMENTATION PAGE

READ INSTRUCTIONS BEFORE COMPLETING FORM

1. REPORT NUMBER: ECOM-4468	2. GOVT ACCESSION NO.
3. RECIPIENT'S CATALOG NUMBER	
4. TITLE (and Subtitle): A HIGHLY-STRESSED CYLINDRICAL ELECTRODE CARBON DIOXIDE (CO_2) TRANSVERSELY EXCITED ATMOSPHERIC (TEA) LASER,	5. TYPE OF REPORT & PERIOD COVERED: Final Technical Report.
	6. PERFORMING ORG. REPORT NUMBER
7. AUTHOR(s): G. R. Osche and H. E. Sonntag	8. CONTRACT OR GRANT NUMBER(s)
9. PERFORMING ORGANIZATION NAME AND ADDRESS: US Army Electronics Command, ATTN: DRSEL-CT-L, Fort Monmouth, New Jersey	10. PROGRAM ELEMENT, PROJECT, TASK AREA & WORK UNIT NUMBERS: 1T1 61102 AH46 E1 031
11. CONTROLLING OFFICE NAME AND ADDRESS: US Army Electronics Command, ATTN: DRSEL-CT-L, Fort Monmouth, New Jersey	12. REPORT DATE: Feb 1977
	13. NUMBER OF PAGES: 18
14. MONITORING AGENCY NAME & ADDRESS (if different from Controlling Office): US Army Electronics Command, ATTN: DRSEL-CT-L, Fort Monmouth, New Jersey 24p.	15. SECURITY CLASS. (of this report): Unclassified
	15a. DECLASSIFICATION/DOWNGRADING SCHEDULE

16. DISTRIBUTION STATEMENT (of this Report)

Distribution Unlimited; Approved for Public Release.

DDC RECEIVED MAR 28 1977 C

17. DISTRIBUTION STATEMENT (of the abstract entered in Block 20, if different from Report)

1T161102AH46

18. SUPPLEMENTARY NOTES

E1

19. KEY WORDS (Continue on reverse side if necessary and identify by block number)

Lasers, Electronics, Pulsed, High-Pressure Modes, Discharges

20. ABSTRACT (Continue on reverse side if necessary and identify by block number)

A cylindrical electrode scheme which utilizes a fine wire as the central electrode is investigated for compact carbon dioxide (CO_2), transversely excited atmospheric (TEA) laser applications. It is found that the strong radial dependence of electrical energy deposition into the plasma, a consequence of the large ratio of outer to inner electrode radii, produces a radial gain profile which is well localized in the center of the discharge tube.

DD FORM 1 JAN 73 1473 EDITION OF 1 NOV 65 IS OBSOLETE

UNCLASSIFIED

037620 SECURITY CLASSIFICATION OF THIS PAGE (When Data Entered)

This allows for efficient matching of low order stable modes to the active gain region while providing a high degree of mode selectivity in favor of these modes. Oscillation in the TEM_{01} Laguerre-Gaussian mode has been obtained at electrical efficiencies approaching 4 percent.

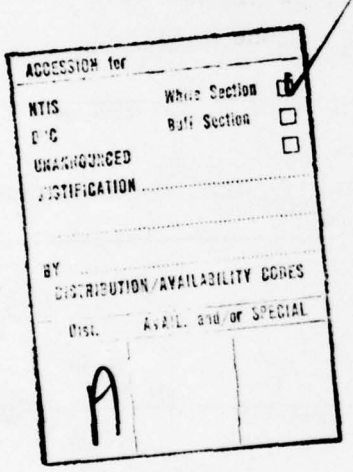

TABLE OF CONTENTS

FIGURES

TABLE OF CONTENTS

A HIGHLY-STRESSED CYLINDRICAL ELECTRODE CO_2 TEA LASER

1. INTRODUCTION

In contrast to current efforts to scale carbon dioxide (CO_2), Transversely Excited Atmospheric (TEA) lasers to larger active volumes, certain applications, both military and commercial, require simple, compact devices. Output energies on the order of 50-100 mJ are usually sought with active volumes on the order of 10-20 cm^3. Attempts to scale down double discharge flat electrode schemes or pin electrode schemes having rectangular apertures are usually confronted with the problem of matching the more common circularly symmetric optical modes to the rectangular active area. This mismatch limits single mode electrical efficiencies to values considerably lower than the corresponding multimode values.[1] In addition, it is observed that arcing problems become more pronounced for small scale TEA discharges. This is attributable, at least in part, to the proportionate increase of field gradients associated with small electrodes which are fabricated to the same tolerances as larger electrodes.

This report describes, in greater detail,[2] a cylindrical electrode scheme for low energy applications which utilizes a small diameter wire as the central electrode. Cylindrical electrodes have been investigated previously for CO_2 TEA laser applications but have always employed large diameter rods as the central electrode.[3,4] These devices necessarily operate in high order transverse modes, unless special toric cavities are employed,[3] and require preionization schemes similar to those of planar electrode geometries. By contrast, a highly-stressed central electrode may be used simultaneously as a preionizing electrode while permitting oscillation of low order transverse modes. In addition, the divergent nature of the current density allows one to achieve relatively high values of volumetric energy deposition in a localized region of the discharge without excessively loading the entire plasma to the point of arcing. An especially attractive feature of the device is its simplicity of construction and maintenance free operation.

2. DESCRIPTION OF ELECTRODES

The electrodes were constructed using a 0.0127 cm (5 mil) diameter tungsten wire and a 1.524 cm i.d. stainless steel vacuum tube (rolled). Figure 1 shows a photograph of the device. Other than a slight flairing of the ends of the tube, which helped reduce field gradients near the edges,

---

1. D. S. Stark, P. H. Cross, and H. Foster, "A Compact Sealed Pulsed CO_2 TEA Laser," IEEE Journal of Quantum Electronics, VOL QE-11, No. 9, Sept 1975, p 774.

2. G. R. Osche and H. E. Sonntag, "A Compact Cylindrical CO_2 TEA Laser," IEEE Journal of Quantum Electronics, QE-12 , Dec 1976, p 752.

3. L. W. Casperson and M. S. Shekhani, "Mode Properties of Annular Gain Lasers," Applied Optics, VOL 14, No. 11, Nov 1975, p 2653.

4. R. K. Garnsworthy, L.E.S. Mathias and C.H.H. Carmichael, "Atmospheric Pressure Pulsed CO_2 Laser Utilizing Preionization by High Energy Electronics," Applied Physics Letters, VOL 19, p 506 (1971).

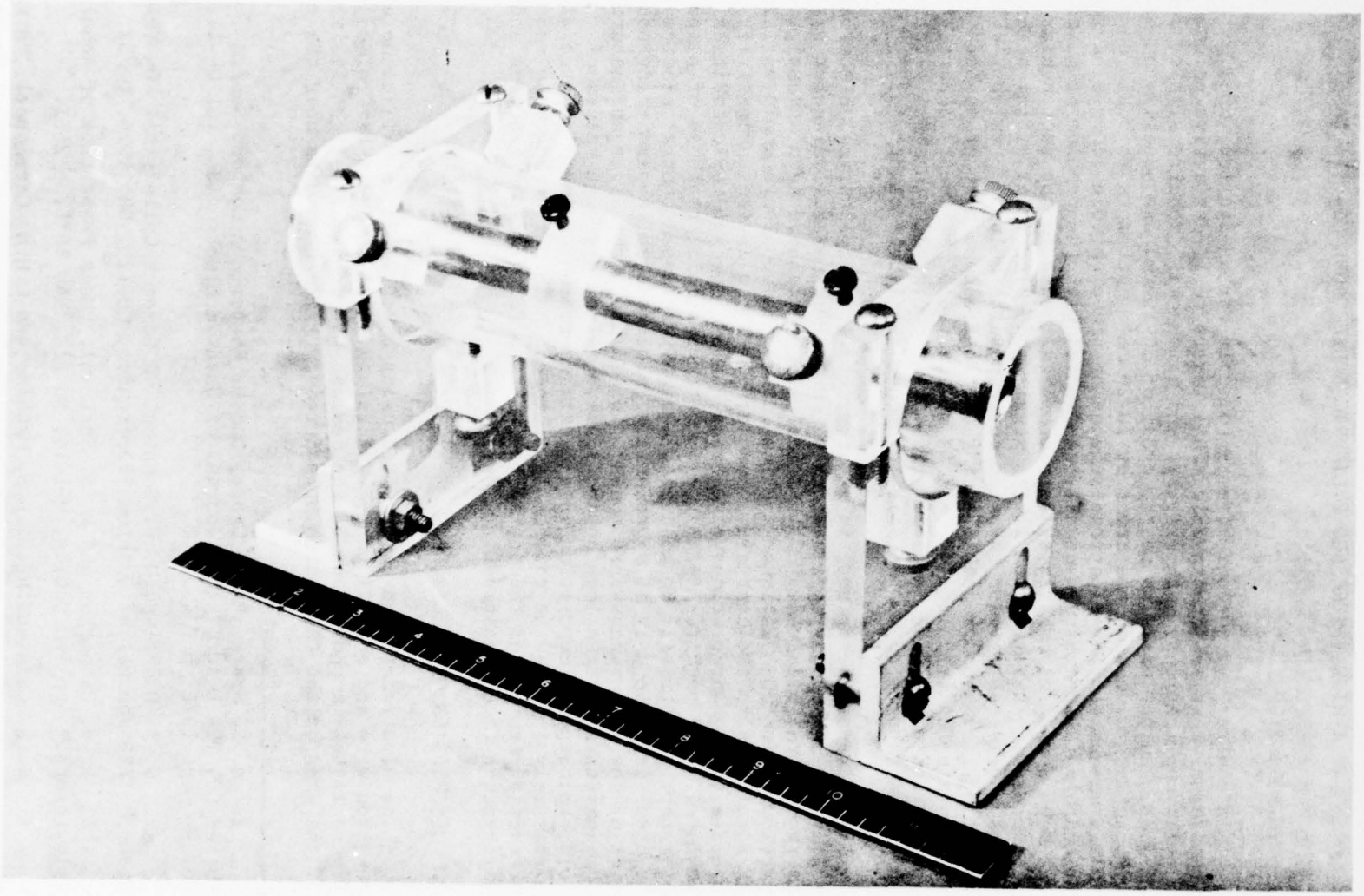

Figure 1. Photograph of laboratory model less mirrors and wire. Note three point adjustments for centering tube about the wire. Tube shown is a shorter version of the one discussed in the text.

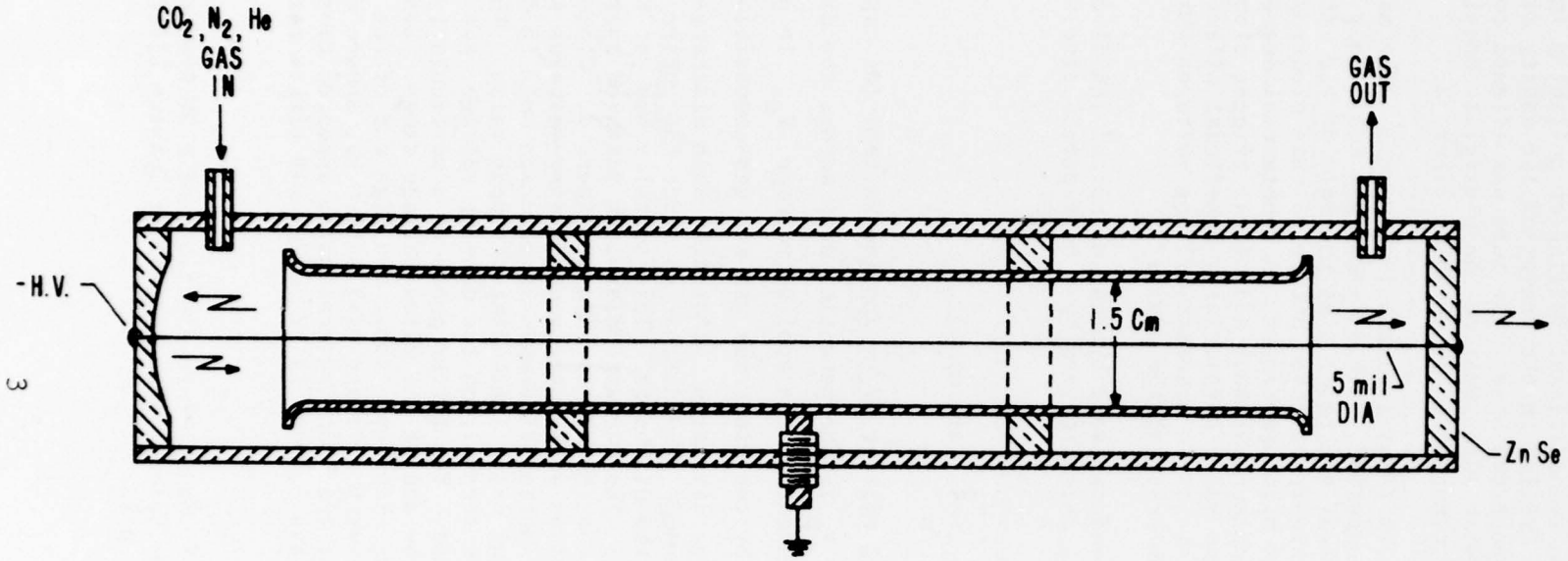

Figure 2. Schematic of a more compact version of cylindrical laser.

these materials did not require additional buffing or polishing in order to prevent arcing. Holes were drilled in the center of the cavity mirrors which were then used to support the wire. The tube was aligned coaxially with the wire via a three-point adjustment on the plexiglass housing. A more compact model might be constructed as shown in Figure 2.

The pulse forming network (PFN) is shown in Figure 3. The main capacitor was 0.01 uF. As expected, stable discharges could only be obtained by letting the central electrode play the role of the cathode. Advantage was taken of the highly stressed nature of this electrode by series triggering the spark gap and main electrodes. A substantial degree of preionization was thereby achieved without additional trigger electrodes or circuitry. This technique had a particularly beneficial affect on the stability of the discharge at low to moderate driving voltages while greatly simplifying the overall complexity of the device.

Current and voltage waveforms were typical of pulsed TEA discharges, the current pulse being well characterized by a half-period sine wave,[5] for example,

$$i(t) = \frac{V_p - V_o}{Z_o} \sin \omega t \qquad (1)$$

where V_p = plasma sustaining voltage, V_o = applied voltage (on capacitors) and $Z_o = (L/c)^{\frac{1}{2}}$. Note that V_p is the potential drop across the discharge which is a constant, independent of the applied voltage, V_o. In particular, V_p is determined primarily by the electrode gap and gas composition as is characteristic of a glow type discharge. (Actually such discharges may be more aptly described as abnormal glow discharges since the entire electrode surface is utilized during the discharge. This subtilty has yet to be fully resolved in the literature.) The current pulsewidth measured approximately 300 ns full-width-half-maximum (FWHM), as seen in Figure 4. Close inspection of a sequence of current pulses at a variety of driving voltages shows that the approximation of a half-period sine-wave is accurate only in describing the first half of the current pulse, including its peak value. The tail of the current pulse depends strongly on the driving voltage, gas mixture, and particular spark gap used. The latter produces a particularly long current gail when operated at the low end of its rated voltage range. Best results were obtained when operating at or even above the high end of the rated voltage range. An EGG 20B, with a rating of 3.5-11.0 kV, showed excellent performance near 14 kV. The resultant current pulse appeared closely approximated by half period sine wave. Above 14 kV an EGG 14B with a rating of 12-36 was used.

---

5. O. P. Judd and J. Y. Wada, "Investigations of a UV Preionized Electrical Discharge and CO_2 Laser," IEEE Journal of Quantum Electronics, VOL QE-10, No. 1, Jan 1974, p 12.

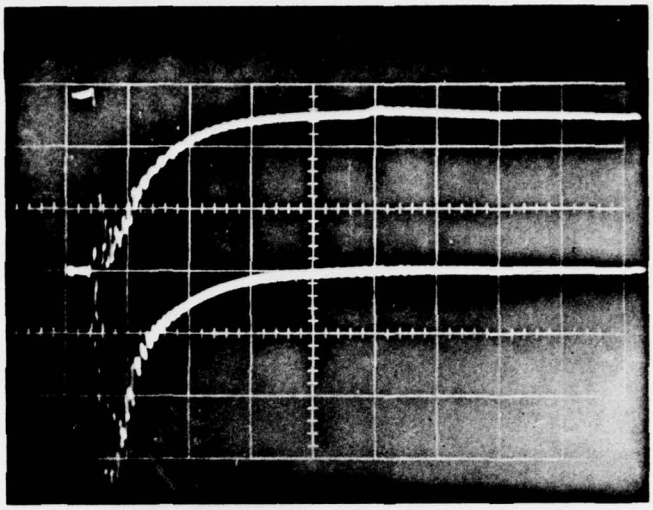

Figure 3. Voltage - current waveforms. Upper trace - 200 V/cm; Lower trace - 50 amps/cm.

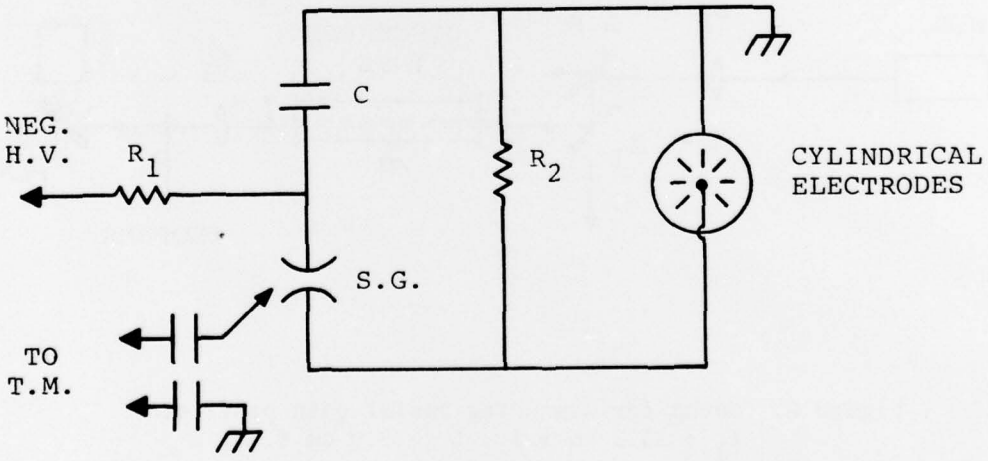

Figure 4. Series triggered PFN. C_1 = 0.01 uF, R_1 = 1.5 M, R_2 = 1 M, T. M. represents trigger module and S. G. represents the spark gap.

Figure 5. End view of discharge. Bright area on top is due to over-exposure of film by wire as viewed slightly downward. Note radial streamers characteristic of high-pressure discharges.

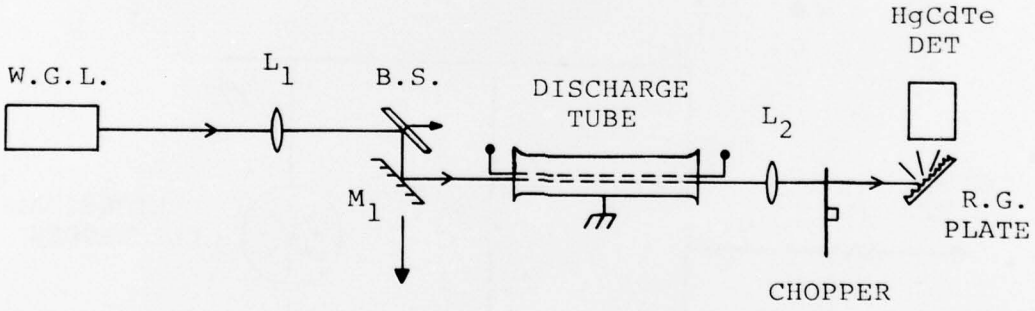

Figure 6. Setup for measuring radial gain profile.
L_1 = 33.2 cm f.l., L_2 = 5.0 cm f.l.,
M_1 = movable mirror, R.G. is rough ground (plate).

Stable discharges could be obtained over a wide range of gas pressures (up to 2.5 atm), gas mixtures (pure N_2, CO_2 or He) and applied voltages (5 to 25 kV). Figure 5 shows a photograph of the discharge as observed from the end of the tube. The presence of "streamers" is quite evident and are characteristic of strongly driven high pressure pulsed glow discharges. Note that their density (number of streamers per unit area) decrease in accordance with the cylindrical geometry. Arcing was found to occur at input energy densities of approximately 30 J/l for a variety of tube lengths (20 cm to 50 cm). Although this value is small compared to that achieved with planar electrodes, it should be kept in mind that the discharge has a strong radial dependence which, as will be shown, allows one to regain the higher values in a limited region of the discharge. Subsequent data to be presented refers to a flowing gas mixture of 1:1:3, CO_2:H_2:He at atmospheric pressure and a tube length of 48.26 cm.

3. RADIAL GAIN PROFILE

In order to perform a meaningful comparison of the present electrode configuration with existing schemes, a detailed understanding of the radial gain profile is required. Small signal gain measurements were made using the setup shown in Figure 6. A 1.63 mm square aperture CO_2 waveguide laser, operating at 120 Torr, was used as the probe laser. The laser oscillated on the P(20), 10.59 um line and had a TEM_{oo} transverse mode. The beam was scanned across the radius of the discharge tube with a moving mirror. A 50 MHz bandwidth HgCdTe detector observed the scattered probe radiation from a rough ground plate, the latter being necessary to minimize beam steering effects caused by thermal lensing and shockwaves. These effects appeared somewhat enhanced compared to those arising from flat electrode schemes due to the large gradients associated with the cylindrical geometry.

The maximum probe beam diameter was measured and found to be approximately 2.5 mm at the ends of the discharge tube; the beam waist after lens L_1 being located halfway into the tube and approximately 2 mm in diameter. The beam was attenuated to approximately 100 mW through a ZnSe beam splitter in order to avoid saturation effects. Since the beam diameter was a sizeable fraction of the tube radius, each measurement constituted an average value of the gain over the probe beam diameter. (Attempts to illuminate the entire tube radius with an expanded probe beam, while scanning the exit beam with a pin-hole/detector arrangement, proved less successful due to diffraction at the tube ends). A chopper was placed at the focal point of lens L_2 and was synchronized with the discharge pulse so that the reference beam could be continuously monitored. This eliminated the problem of long term amplitude stability of the probe laser.

A typical oscilloscope trace of a gain measurement for some value of r/b is shown in Figure 7. The relatively high value of the low frequency cutoff of the detector circuitry (10 kHz) resulted in a differentiated square wave for the chopped probe beam. The rise and fall portions of the square wave appear as positive and negative going pulses at the beginning and end of the trace. The gain pulse appears near the center. Assuming that the gain pulse shape does not change with the probe location in the discharge,

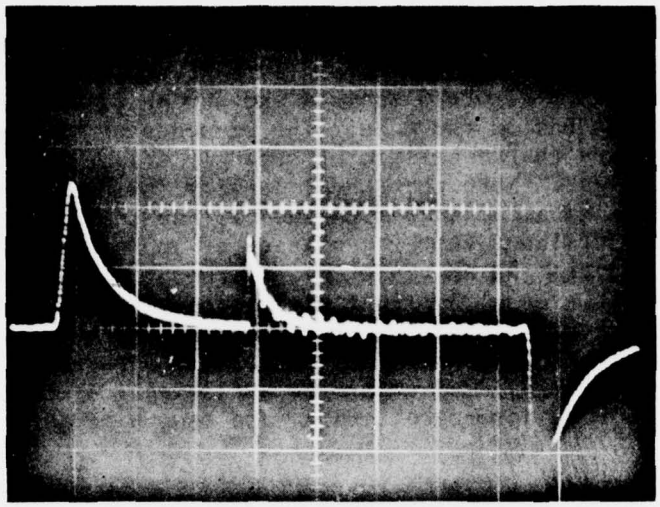

Figure 7. Gain and probe signal. Sweep speed = 100 usec/cm.

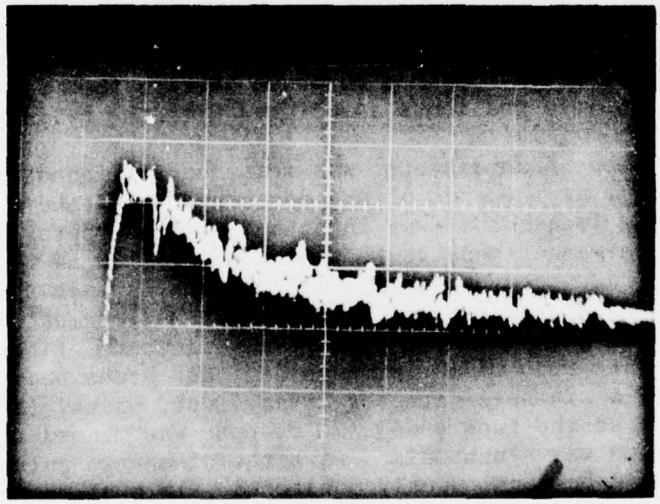

Figure 8. Expanded view of gain pulse - 20 usec/cm.

which is certainly reasonable, values of gain normalized to the peak value may be readily obtained via such measurements.

Figure 8 is an expanded view of the gain pulse. Considerable structure of a quasi-periodic nature is to be seen in both figures. This structure is attributable to acoustic shock waves generated by the current pulse bouncing between electrodes and thereby perturbing the probe beam. For an electrode gap of 0.762 cm and a sound velocity of approximately 33,500 cm/sec, a transmit time of 22.5 usec results which agrees closely with the observed spacing.

Values of gain in dB/m were obtained by measuring the output probe and peak gain signal ($I_2 + I_2$) and the input probe intensity (I_1) and using the relation

$$g = \frac{10}{L} \log \frac{(I_2 + I_2')}{I_1} \qquad (2)$$

where L is the active gain length (48.26 cm).

The resultant gain profile, normalized to the outer electrode radius, b, is shown in Figure 9. Values obtained near the inner electrode surface at r = a were complicated by diffraction effects arising from the partial obstruction of the probe beam by the wire and its support. However, since this data point was found to be reproducible, it is included with a reasonable amount of confidence. Values obtained near r = b were very low and essentially undetectable within the accuracy of the setup. Peak gains of 5-6 dB/m were observed at high input energies (2 to 2.5 J) in the vicinity of the central electrode.

An idealized qualitative understanding of the radial gain profile may be obtained by considering the radial dependence of such parameters as, E/p, current density, j, and energy deposition, jE, for a cylindrical geometry. These quantities, appropriately normalized, are plotted in Figure 9 and are discussed below.

From Gauss's law we obtain

$$\frac{E}{p} = \frac{V_p - V_c}{p \ln b/a} \cdot \frac{1}{r} \qquad (3)$$

where V_c is the cathode potential drop and p is the pressure in atmospheres. Here V_c has been corrected for the cathode potential drop which was assumed to be p_{300} volts. Possible effects due to space charge formation are neglected for simplicity. From the work of Nighan[6] and Judd,[7] we see that

6. W. L. Nighan, "Electron Energy Distributions and Collision Rates in Electrically Excited N_2, CO, and CO_2," Physical Review A, VOL 2, No. 5, Nov 1970, p 1989.

7. O. P. Judd, "The Effect of Gas Mixture on the Electron Kinetics in the Electrical CO_2 Gas Laser," Journal of Applied Physics, VOL 45, No. 10, Oct 1974, p 4572.

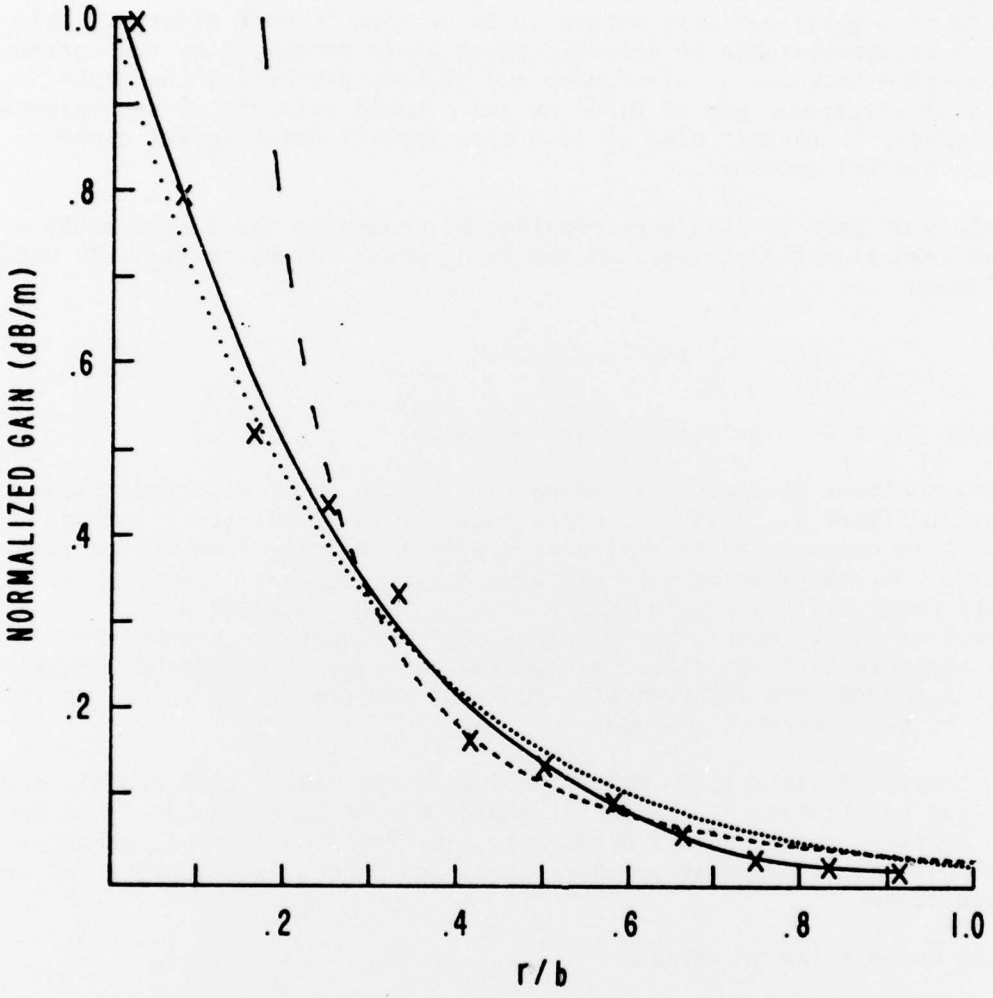

Figure 9. Radial gain profile (dB/m) as given by $g = \frac{10}{L} \log \frac{I}{I_o}$. Results are normalized to peak value. Largest gains observed were 5-6 dB/m near r = a. Gas ratios were CO_2, N_2, He = 1:1:3. Dashed curve represents $\alpha(r/b)^{-2}$ with $\alpha = 0.03$. Dotted curve represents $e^{-\beta r/b}$, $\beta = 3.7$.

optimum values of E/p for pumping CO_2 and N_2 exists at about r/b = 0.25 (E/p = 5.2 kV/cm atm), while for values below r/b = 0.1 (E/p = 12.9 kV/cm atm) a significant fraction of the available electrical energy is used for electronic excitation, dissociation, and ionization. The latter is, of course, necessary in order to sustain the discharge, whereas the former two constitute a loss for the system. On the other hand, the current density

$$j(t) = \frac{i(t)}{2\pi Lr} \tag{4}$$

increases rapidly below r/b = 0.15 and more than compensates for the less efficient pumping of CO_2 and N_2 in this region. The combined effect of both E/p and j is therefore to produce a radial gain profile which is largest near the wire but which falls off slower than the r^{-2} dependence of jE (see Equations (6) and (7) below). This is easily seen by noting the dashed curve in Figure 9 which represents a best fit of $\alpha(r/b)^{-2}$ (α = 0.03) to the observed data. Of course, a more exact analysis would require the inclusion of space charge effects since they could significantly alter the radial dependences of j and E in jE. A theoretical calculation of the radial gain profile, based on the works of Nighan and Judd, will be the subject of later work.

An interesting and possibly useful representation of the observed gain profile is

$$g = g_o e^{-\beta r/b} \tag{5}$$

where g_o is the peak small signal gain at the wire and β = 3.7. This expression is plotted in Figure 9 as a dotted curve and is seen to closely approximate the observed profile. At higher currents it is expected that the gain curve flattens somewhat since the central regions saturate before the outer regions. This was not the case for the data points of Figure 9, however, since they corresponded to a peak current of 200A which, for r/b = 0.1, resulted in the still moderate value of 8.66 A/cm^2.

The instantaneous electrical energy deposited in the plasma is given by

$$jE = \frac{V_p(t)i(t)}{2\pi L \ln B/a} \cdot \frac{1}{r^2} . \tag{6}$$

Integrating from $0 \rightarrow \pi$, we obtain the radial distribution of the total energy, E_t, i.e.,

$$E_T(r) = \frac{E_T}{2\pi L \ln b/a} \cdot \frac{1}{r^2} . \tag{7}$$

Referring to Figure 10 we see that relatively large input energy densities may be obtained in a localized region of the plasma. For example, at r/b = 0.1 and an input energy of 2J, a value of 238 J/l is obtained with a corresponding value for E/p of 12.9 kV/cm atm. At r/b = 0.135, 131 J/l is obtained at 9.6 kV/cm atm. This should be compared with the reported results of a UV preionized laser,[5] which attained a maximum value of 150 J/l at 9.5 kV/cm atm.

The significance of the r^{-2} dependence of jE is better appreciated by integrating Eq. (7) over a cylindrical volume element extending from r = a to r = r. Normalizing to E_t, one finds

$$K = 1 + \frac{\ln r/b}{\ln b/a} \tag{8}$$

which represents that fraction of the total energy deposited within the normalized radius r/b (see Figure 10). One sees that as a consequence of the large value of b/a, approximately 85 percent of the available electrical energy is deposited within r/b = 0.5, or within 1/4 of the total gas volume. By comparison, the gain falls off by approximately 85 percent within this same radius so that the point r/b = 0.5 becomes a meaningful boundary for characterizing the extent of the usable gain region. For the present device this amounts to approximately 22 cm^3 of active volume.

4. LASER OUTPUT CHARACTERISTICS

The small active gain area associated with the present configuration suggests that the system may be efficiently matched to low order transverse modes of stable optical cavities. In addition, the strong radial gain profile should provide some degree of mode selectivity in favor of low order modes. In order to investigate these possibilities, a plane-concave cavity was employed which had a radius of curvature R = 3.8 meters and a cavity length d = 55 cm. Coarse mirror alignment was achieved via a helium-neon laser which entered off-axis through the ZnSe output mirror. The entire mirror-wire system was considered aligned when the lowest order transverse mode appeared. At low to moderate driving voltages, oscillation occured in what appeared to be the TEM_{01} Laguerre-Gaussian mode. In general, the intensity distributions of the set of Laguerre-Gaussian modes are given by [8]

$$|\Psi_{mn}|^2 = \frac{2r^2}{w^2} \left| L_m^n \left(\frac{2r^2}{w^2}\right) \right|^2 e^{-\frac{2r^2}{w^2}} \tag{9}$$

where L_m^n are the generalized Laguerre polynominals of order m and index n. These modes scale according to the well known beam parameter equations[8]

---

8. H. Kogelnik and T. Li, "Laser Beams and Resonators," Applied Optics, VOL 5, No. 10, Oct 1966, p 1550.

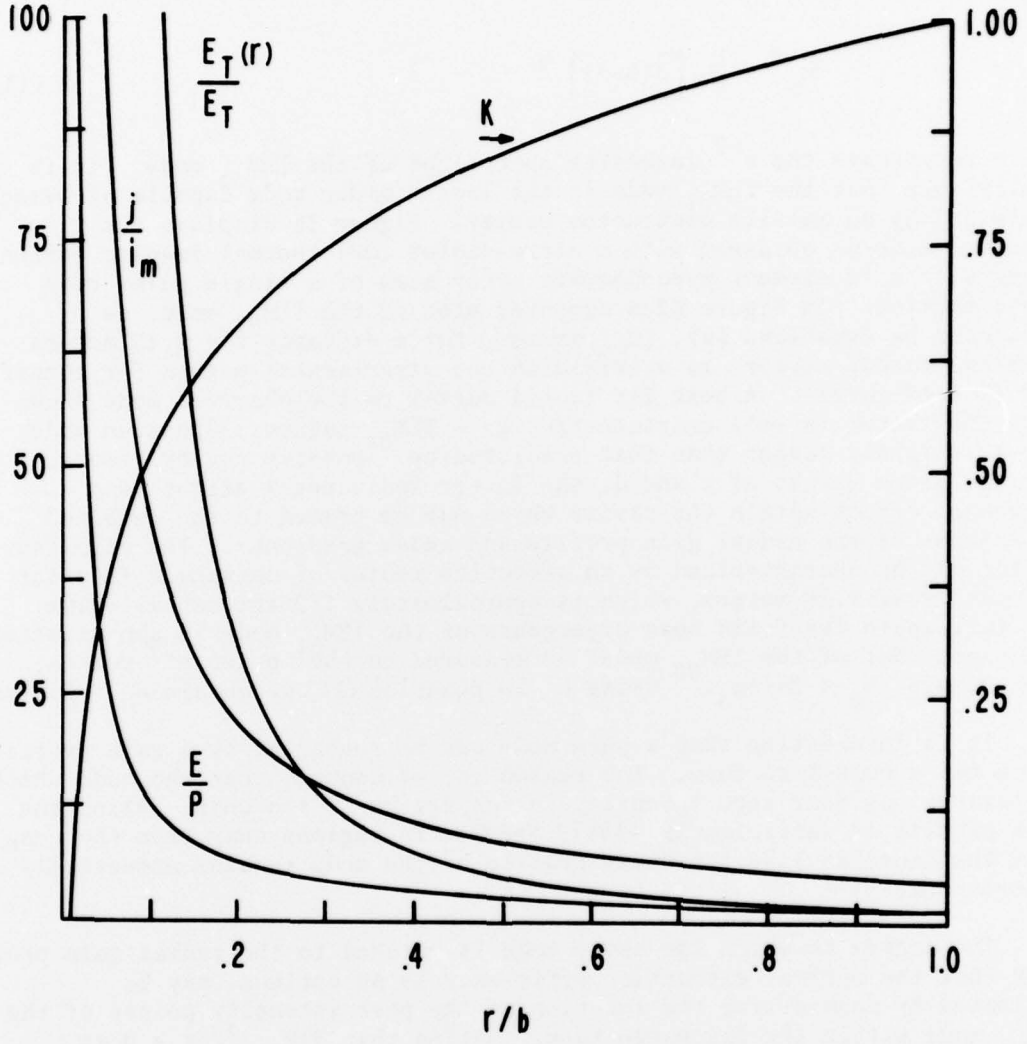

Figure 10. Idealized curves characterizing highly stressed, coaxial discharge.

(K) = dimensionless, $(\frac{E}{p}) = \frac{kV}{cm\ atm}$.

$(J/i_m) = cm^{-2} \times 10^3$, $(E_T(r)/E_T) = liter^{-1}$.

K corresponds to right ordinate. All others, the left ordinate.

$$w^2(z) = w_o^2 \left\{ 1 + \left(\frac{\lambda z}{\pi w_o^2} \right)^2 \right\} \qquad (10)$$

and

$$w_o^2 = \frac{\lambda}{\pi} \left[d(R-d) \right]^{1/2} \qquad (11)$$

which represents the e^{-2} intensity spot sizes of the TEM_{oo} mode. It is easily seen that the TEM_{01} mode is the lowest order mode capable of being sustained by an axially obstructed cavity. Figure 11 displays the observed mode as obtained with a ultra-violet (UV) thermal imaging screen along with a 16 element pyroelectric array scan of a single pulse beam cross section. In Figure 12 a computer plot of the TEM_{01} mode, as predicted by Equations (9), (10), and (11) for a distance $z = 2.15$ meters from the output mirror, is overlaid on the experimental points for comparison (dotted curve). A best fit (solid curve) to the observed mode shows that the latter is well characterized by a TEM_{01} Laguerre-Gaussian mode, but is slightly larger than that predicted by passive cavity theory. For the given values of z and d, the latter indicates a slight beam narrowing effect within the cavity which may be traced to the combined influences of the radial gain profile and index gradients. The resultant effect may be characterized by an effective radius of curvature (R') for the cavity of 1.89 meters, which is approximately 1/2 the actual value. The full-angle far-field beam divergence of the TEM_{01} mode is approximately 1.5 times that of the TEM_{00} mode[9] as measured to the outer e^{-2} points, for example, $\theta_d = 3\lambda/\pi\omega_o$. Using R' in Equation (11) we obtain $\theta_D = 5.9$ mrad.

It is interesting that a pure mode can be sustained by a gain profile which has a cusp-like form. The reason is, of course, that the mode which oscillates has near zero intensity in the region of the cusp. Also, the gain profile is sufficiently slowly varying in regions away from the cusp that the Gaussian-like intensity profile of the mode remains essentially umperturbed.[10,11]

The degree to which the above mode is matched to the radial gain profile, such that the optical extraction efficiency is an optimum, may be estimated by considering the location of the peak intensity points of the TEM_{01} mode within the discharge tube. Noting that $d|\Psi_{01}|^2/dr = 0$ at $r = w/\sqrt{2}$ for all z, we find that the peak intensity at the output mirror for the observed mode occurs at $r = 0.120$ cm (confirmed with a UV screen), and $r = 0.143$ cm at the rear mirror. These points correspond to the

9. R. J. Freiberg and A. S. Halsted, "Properties of Low Order Transverse Modes in Argon Ion Lasers," Applied Optics, VOL 8, No. 2, Feb 1969, p 355.

10. L. W. Casperson, "Gaussian Light Beams in Inhomogeneous Media," Applied Optics, VOL 12, No. 10, Oct 1973, p 2434.

11. H. Kogelnik, "On the Propagation of Gaussian Beams of Light Through Lens Like Media Including Those with a Loss or Gain Variation," Applied Optics, VOL 4, No. 12, December 1965, p 1562.

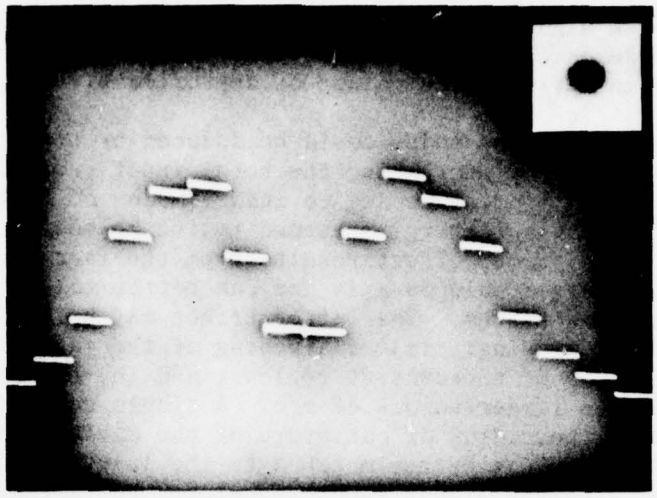

Figure 11. Pyroelectric array scan of single pulse beam profile at z = 2.15 m. Distance between data points corresponds to 1.1 mm.

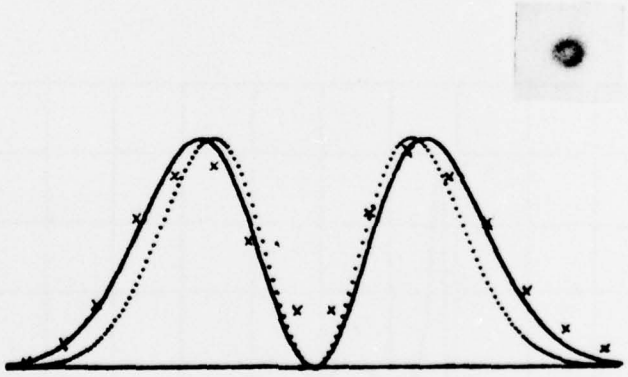

Figure 12. Comparison of theory and experiment. Dotted curve represents idealized passive cavity theory. Solid curve represents best fit of passive cavity mode to experimental points.

normalized radii in Figure 9 of r/b = 0.157 and 0.188, respectively, which are well within the high gain region. For additional comparison, the e^{-2} points of this mode extend to r/b = 0.335 and 0.398, respectively, corresponding to an optical mode volume of approximately 11 cm^3.

Higher order transverse modes could be induced by slightly misaligning the cavity (or wire) or by increasing the total input energy. It was found that cavity misalignment tended to induce modes of higher azimuthal index, n, while large input energies tended to induce modes of higher radial index, m. The former effect results from the fact that the higher order modes have a larger hole on-axis and can better tolerate the misaligned cavity-wire system. The latter effect may be explained as a combination of the following: (a) flattening of the gain profile due to saturation by the pump of the central regions, and (b) the extension of the usable gain region to larger values of r/b. A simple test of the latter involved increasing the radius of curvature of the cavity mirror such that the TEM_{01} mode diameter was better matched to the larger active gain region associated with the higher input energies. For a radius of curvature of 8 meters, it was found that this mode again became the more dominant one. Other modes observed included TEM_{02}, TEM_{03}, and TEM_{11}.

The laser pulse, as measured with a 50 MHz HgCdTe detector, was typical of CO_2, N_2, He TEA lasers consisting of an initial 100 nsec spike followed by 1 usec tail (see Figure 13). The energy per pulse was calculated from an average power measurement made at a repetition rate of 10 Hz.

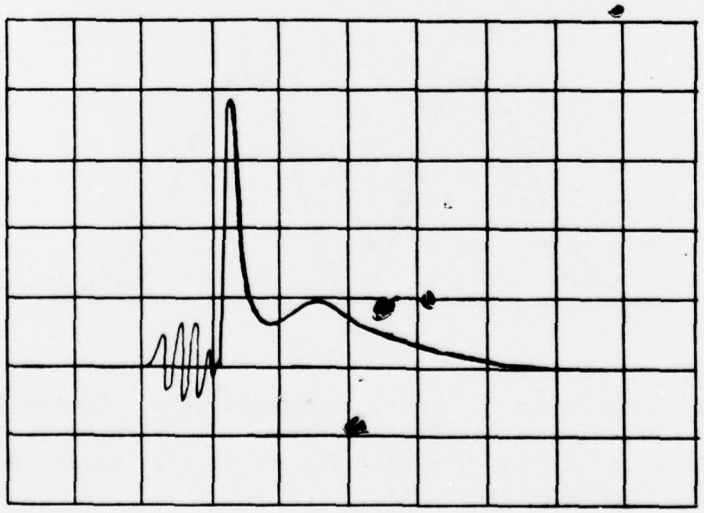

Figure 13. Laser output pulse- 0.5usec/cm. Photograph is redrawn for clarity.

The results are shown in Figure 14. The input energy corresponds to the energy in the capacitor, $\frac{1}{2} CV_o^2$. The linear nature of the curve is assumed to be due to the non-uniform energy deposition (r^{-2}) which is capable of saturating only a limited portion of the active gain region. The total electrical-to-optical conversion efficiency is seen to approach 4 percent at the high end of the curve. This value exceeds slightly that achieved with planar electrode geometries mainly due to the better utilization of active volume. For example, in Reference 1 a drop in electrical efficiency from approximately 10 percent to approximately 3 percent was realized when the device was apertured for single mode operation. The resultant optical mode volume corresponded to only 55 percent of the usable gain volume. It is expected that the values reported here could be improved still further by optimally coupling the cavity and by adjusting cavity parameters and electrode radii to further optimize the optical extraction efficiency.

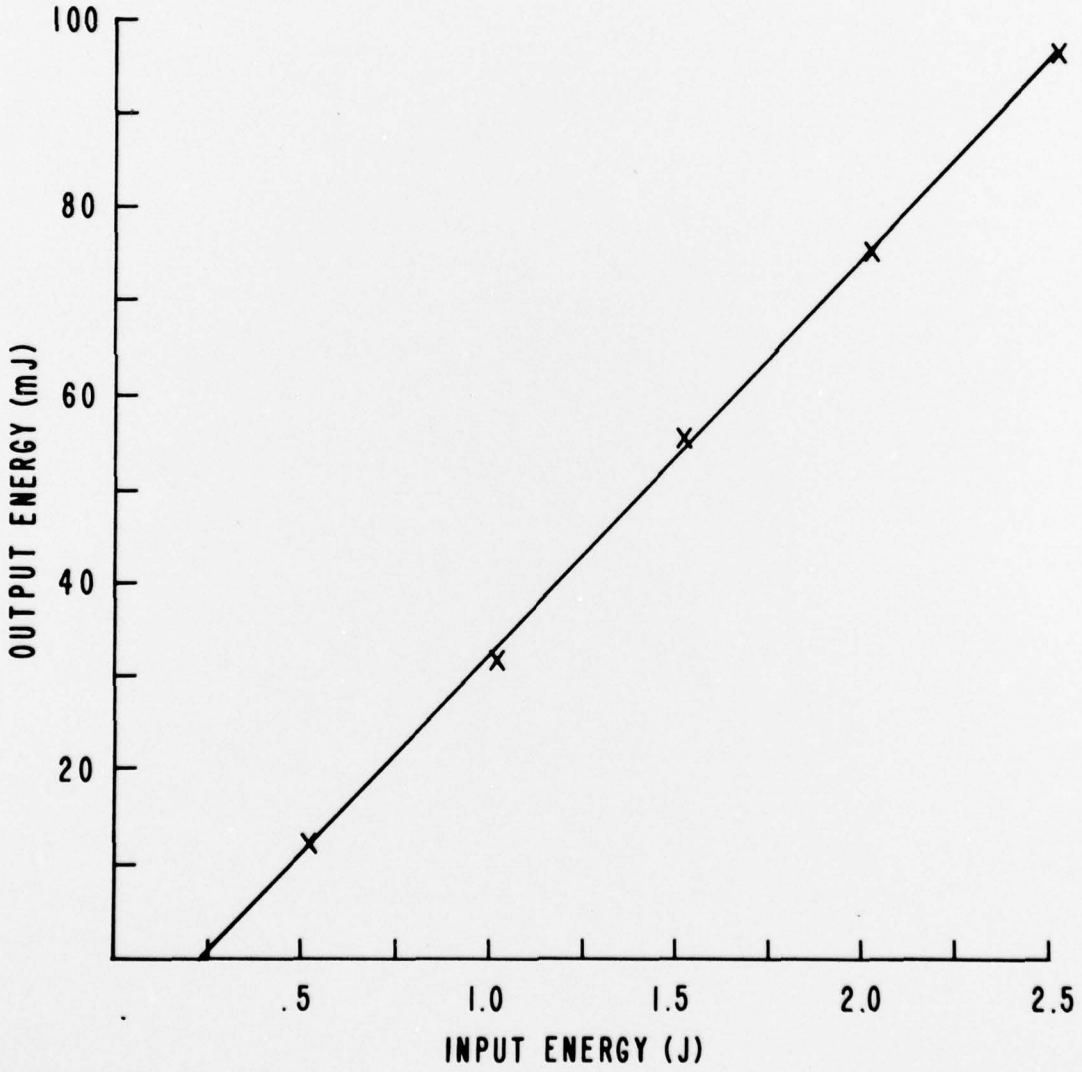

Figure 14. Energy output versus energy input for 48.3 cm active length. Output mirror reflectivity was 89 percent. Data points were obtained with a power meter at 10 pps. Input energy = $\frac{1}{2} CV_o^2$.

5. SUMMARY AND CONCLUSIONS

It has been shown that a highly-stressed cylindrical electrode geometry exhibits several useful characteristics for low energy CO_2 TEA laser applications. Most important is the fact that low order stable optical modes (TEM_{01}) may be obtained without aperturing at electrical efficiencies near 4 percent. In addition, the device is simple to construct and has demonstrated reliable arc free operation for a minimum of electrode preparation. It is expected that this geometry should also be useful in exciting other molecular gas systems such as DF/HF chemical lasers.